INL/CON-05-00508
PREPRINT

Modeling Permeability in Coal Using Sorption-Induced Strain Data

2005 SPE Annual Conference and Technical Exhibition

Eric P. Robertson
Richard L. Christiansen

October 2005

The INL is a
U.S. Department of Energy
National Laboratory
operated by
Battelle Energy Alliance

Modeling Permeability in Coal Using Sorption-Induced Strain Data

Eric P. Robertson, SPE, Idaho National Laboratory and Richard L. Christiansen, SPE, Colorado School of Mines

Abstract

Sorption-induced strain and permeability were measured as a function of pore pressure using subbituminous coal from the Powder River basin of Wyoming, U.S.A. and high-volatile bituminous coal from the Uinta-Piceance basin of Utah, U.S.A. We found that for these coal samples, cleat compressibility was not constant, but variable. Calculated variable cleat-compressibility constants were found to correlate well with previously published data for other coals. Sorption-induced matrix strain (shrinkage/swelling) was measured on unconstrained samples for different gases: carbon dioxide, methane, and nitrogen. During permeability tests, sorption-induced matrix shrinkage was clearly demonstrated by higher permeability values at lower pore pressures while holding overburden pressure constant; this effect was more pronounced when gases with higher adsorption isotherms such as carbon dioxide were used. Measured permeability data were modeled using three different permeability models that take into account sorption-induced matrix strain. We found that when the measured strain data were applied, all three models poorly matched the measured permeability results. However, by applying an experimentally derived expression to the strain data that accounts for the constraining stress of overburden pressure, pore pressure, coal type, and gas type; two of the models were greatly improved.

Introduction

Coal seams have the capacity to adsorb large amounts of gases because of their typically large internal surface area (30 m^2/g to 300 m^2/g).[1] Some gases, such as carbon dioxide, have a higher affinity for the coal surfaces than others, such as nitrogen. Knowledge of how the adsorption or desorption of gases affects coal permeability is important not only to operations involving the production of natural gas from coal beds, but is also important to the design and operation of projects to sequester greenhouse gases in coal beds.[2]

As reservoir pressure is lowered, gas molecules are desorbed from the matrix and travel to the cleat (natural fracture) system where they are conveyed to producing wells. Fluid movement in coal is controlled by diffusion in the coal matrix and described by Darcy flow in the fracture (cleat) system. Because diffusion of gases through the matrix is a much slower process than Darcy flow through the fracture (cleat) system, coal seams are treated as fractured reservoirs with respect to fluid flow. However, coalbeds are more complex than other fractured reservoirs because of their ability to adsorb (or desorb) large amounts of gas.

Adsorption of gases by the internal surfaces of coal causes the coal matrix to swell and desorption of gases causes the coal matrix to shrink. The swelling or shrinkage of coal as gas is adsorbed or desorbed is referred to as sorption-induced strain. Sorption-induced strain of the coal matrix causes a change in the width of the cleats or fractures that must be accounted for when modeling permeability changes in the system. A number of permeability-change models[3,4,5,6,7,8] for coal have been proposed that attempt to account for the effect of sorption-induced strain. Accurate measurement of sorption-induced strain becomes important when modeling the effect of gas sorption on coal permeability.

For this work, laboratory measurements of sorption-induced strain were made for two different coals and three gases. Permeability measurements were also made using the same coals and gases under different pressure and stress regimes. The objective of this current work is to present these data and to model the laboratory-generated permeability data using a number of permeability-change models that have been described by other researchers. This work should be of value to those who model coalbed methane fields using reservoir simulators as these results could be incorporated into these reservoir models to improve their accuracy.

Coal Collection and Handling

Coal Description. A number of large coal blocks, roughly one cubic foot in size, were collected from coal mines in Utah and Wyoming. High-volatile bituminous coal from the Uinta-Piceance basin was collected from the Gilson seam of the Book Cliffs coal field from an underground mine near Price, Utah. Subbituminous, low-contaminant coal from the Powder River basin was collected from the Anderson seam from an open pit coal mine near Gillette, Wyoming. At the mine location, the Anderson seam was over 100 ft thick. Proximate, ultimate, and heating value analyses were subsequently done on samples of the collected coal and are shown in Table 1.

Table 1. Properties of coal samples collected and used in this research as ascertained from various analyses on an "as received" basis.

	Anderson	Gilson
Location of seam	Wyoming	Utah
Coal rank	Subbituminous	High-volatile bituminous
Proximate Analysis wt%:		
Moisture	26.60	7.52
Ash	6.18	2.99
Volatile Matter	30.99	37.42
Fixed Carbon	36.23	52.07
Total	100.00	100.00
Ultimate Analysis wt%:		
Moisture	26.60	7.52
Hydrogen	2.08	3.86
Carbon	50.57	71.66
Nitrogen	0.43	1.36
Sulfur	0.27	0.49
Oxygen	13.87	12.12
Ash	6.18	2.99
Total	100.00	100.00
Heating Value, Btu/lb		
Measured	8,514	12,437
Literature values[9,10]	8,220	12,000
Vitrinite Reflectance, %	0.24	0.53

Coal Collection and Sample Preparation. The Utah coal was taken from the conveyer belt carrying recently mined coal out of the underground mine as close to the active mine face as possible to limit oxygen exposure. Immediately after being taken from the conveyer, each sample was double wrapped in plastic bags and sealed by tape. Transporting the sample from the mine face to the surface took from 5 to 20 minutes depending on the collection site. Upon reaching the surface, the samples were removed from the bags and placed under de-ionized water inside containers for transport back to the Idaho National Laboratory (INL) in Idaho Falls, Idaho.

The Wyoming coal was collected from recently exposed walls from an open pit mine. Large boulders were broken to expose fresh coal inside and smaller samples (roughly one cubic foot) were then taken from this fresh area and immediately placed under water in sealed containers for transport to the INL.

The coal blocks were kept underwater at INL laboratories until needed. The small samples used to measure strain were taken from the larger blocks by using a rock saw cooled by de-ionized water. Cores used to measure permeability were drilled parallel to the bedding plane from the blocks obtained from the mines using de-ionized water as the cooling fluid. Some of the 2-inch diameter cores "fell apart" either while drilling or attempting to remove them from the bit, but persistence and care while drilling resulted in many good cores to use for flow tests. The cores were stored in small, sealed containers under de-ionized water until used in the experiments.

Sorption-Induced Strain Measurements

Strain is a measure of the deformation of a medium as stresses are applied. Volumetric strain is the ratio of the change in volume to the original volume ($\Delta V/V$), while linear strain is the ratio of the change in length to the original length of the sample ($\Delta L/L$).

If a sample had rectangular dimensions, the relationship between volumetric strain and linear strain would be:

$$S_V = S_{L_1} + S_{L_2} + S_{L_3} + S_{L_2}S_{L_3} + S_{L_1}S_{L_3} + S_{L_1}S_{L_2} + S_{L_1}S_{L_2}S_{L_3}, \quad \text{..... (I)}$$

where S_V is volumetric strain, S_L is linear strain and the numbered subscripts represent the three principal dimensions. If the body were isotropic, the strain in all three dimensions would be equal and the relationship between volumetric and linear strain would be:

$$S_V = 3S_L + 3S_L^2 + S_L^3. \quad \text{..... (2)}$$

Further, by assuming a small strain, the final two terms can be neglected and the relationship reduces to:

$$S_V = 3S_L. \quad \text{..... (3)}$$

Sorption-Induced Strain. Sorption-induced strain was measured at 80° F using a newly developed apparatus that can more rapidly equilibrate the coal samples. A description of the apparatus was previously given by Robertson and Christiansen.[11,12] **Fig. 1** shows the results of sorption-induced strain measurements as a function of gas pressure for two different coals and three different gases.

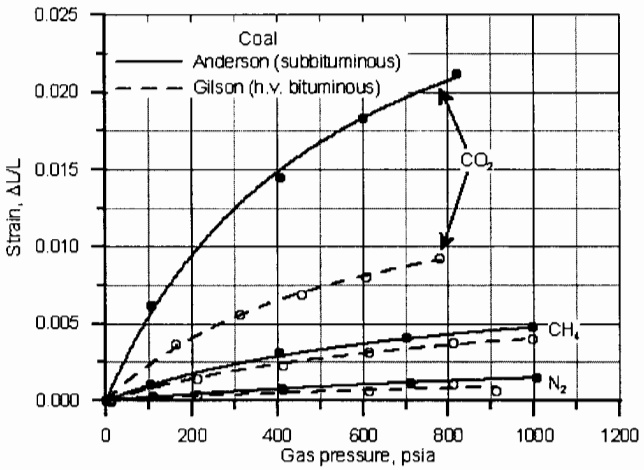

Fig. 1 – Sorption-induced linear strain for two coals and three gases at 80° F.

The lines through the strain data in Fig. 1 are curves fitted using the following Langmuir-type equation:

$$S = S_{max}\frac{p}{p_L + p}, \quad \text{..... (4)}$$

where S is the measured strain, S_{max} (Langmuir strain) is a constant representing the strain at infinite pressure, p is the gas pressure in psia inside the pressure chamber, and p_L (Langmuir pressure) is a constant representing the pressure at which the measured strain equals ½ S_{max}. Not surprisingly, this

Langmuir-type equation has the same form as that used to model adsorption isotherms in coal and fits the data very well.

For both coals used in the study, the strain caused by CO_2 adsorption was the greatest of the three gases tested followed by CH_4 and finally N_2. Based on these sorption-induced strain data, one would expect a lower permeability if CO_2 were the flowing fluid compared to the permeability for N_2. For each gas, the Langmuir pressure, p_L, was similar and increased as the value for S_{max} decreases.

Table 2 shows the strain curve constants used to fit the data in Fig. 1. This table also shows the R^2 value for each of the curves shown in Fig. 1. The high R^2 values shown in this table are an indication that the Langmuir-type equation represented in Eq. (4) provides a very good model for the given strain data.

Table 2. Langmuir constants for sorption-induced strain curves for Anderson and Gilson coals at 80° F.

Gas	Coal	Constants for Strain Curves		R^2 value for curve fit
		Normalized S_{max}	Average p_L, psia	
CO_2	Anderson	0.03527	555.25	0.9984
	Gilson	0.01559		0.9972
CH_4	Anderson	0.00931	886.03	0.9960
	Gilson	0.00765		0.9967
N_2	Anderson	0.00305	1119.93	0.9949
	Gilson	0.00196		0.8639

Permeability Measurements

All permeability measurements were made in INL laboratories at 80° F with gas as the flowing fluid using 2-inch diameter cores. **Fig. 2** is a photograph of the trimmed ends of some Gilson seam cores. This figure is shown to give the reader an idea of a typical cleat system associated with these cores.

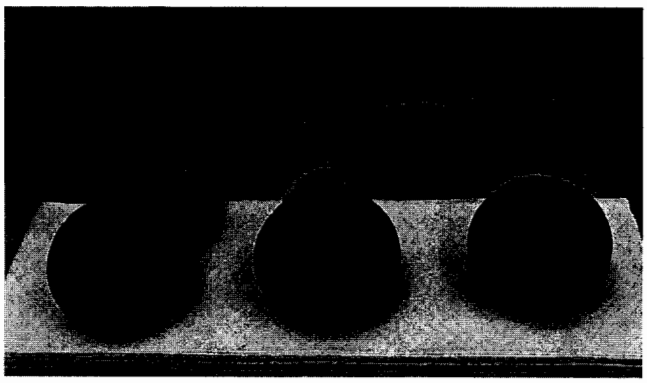

Fig. 2 – Photograph of trimmed ends from Gilson seam coal cores 2 inches in diameter. Note the irregular cleat system associated with this coal.

Permeability Apparatus Description. A hydrostatic-type core holder was used for the permeability experiments. The flowing gas was supplied by pressurized gas cylinders and the flow rate was controlled by adjusting both the cylinder regulator and a metering valve upstream of the core holder. A back pressure regulator was used to apply a minimum of 100 psia of pore pressure in order to minimize the Klinkenberg effect of gas permeability measurements. Upstream and differential pressures were made using pressure transducers. A flow meter was placed directly downstream of the back pressure regulator.

Experimental Procedure. Coal cores used in the permeability experiments were cut under de-ionized water and stored immersed in sealed containers until needed. After removing a core from their sealed storage containers, it was surface dried, measured, wrapped with Teflon and aluminum foil, placed into the hydrostatic core holder set at 80° F (the same temperature as the strain experiments), and allowed to equilibrated for 24 hours inside the core holder with nitrogen flowing through at a low rate.

Varying Overburden Pressure. Achieving a repeatable permeability response was an important part of the preparation of the cores. To do this, the average pore pressure was set and held at a constant 100 psia and the overburden pressure was cycled from 1000 psia down to 300 psia and back up to 1000 psia while measuring permeability changes due to the change in net stress. The flow rate was adjusted as needed to keep the average pore pressure constant.

During the first overburden pressure cycling for a core, there would typically be quite a bit of hysteresis with the permeability data. However, additional pressure overburden pressure cycles reduced the hysteresis until a repeatable permeability curve was obtained as a function of overburden pressure and then the core would be considered ready for data collection.

Varying Pore Pressure. Once the permeabilities of the cores were established and repeatable with a change in overburden pressure, additional experiments were run wherein the pore pressure was varied, allowing gases to be adsorbed or desorbed. Data for these experiments were obtained by setting the overburden pressure at a constant 1000 psia and varying the pore pressure between 100 psia and 800 psia. Because pore pressure was varied, gases were adsorbed or desorbed, and the effects of sorption-induced strain were manifest in the permeability results.

Changing the Flowing Gas. During the course of this project, we studied how sorbing different gases changed permeability. Specifically we considered carbon dioxide, methane, and nitrogen. When an experiment was finished with one gas, helium was then flushed through the core at a low rate for at least 24 hours to desorb any residual sorptive gas left in the core. If permeability were not stable by the end of 24 hours, then additional time would be permitted.

Permeability Models

Three permeability models were selected from the literature to model our laboratory permeability data. Seidle and Huitt[5] published a model in 1995, Palmer and Mansoori[6] published theirs in 1998, and Shi and Durucan[8] published their model in 2003.

A brief explanation of each of the models is laid out in the following paragraphs, but for further details, see their respective papers.

Seidle-Huitt Model. This model begins with the assumption derived by Reiss[13] that the ratio of the current permeability, k, to the initial permeability, k_0, is equal to the cube of the ratio of the current porosity, ϕ, to the initial porosity, ϕ_0:

$$\frac{k}{k_0} = \left(\frac{\phi}{\phi_0}\right)^3 \quad \text{.....(5)}$$

The porosity ratio equation was given as

$$\frac{\phi}{\phi_0} = 1 + \left(1 + \frac{2}{\phi_0}\right) c_m V_m \left(\frac{p_0}{p_L + p_0} - \frac{p}{p_L + p}\right), \quad \text{.....(6)}$$

where $c_m V_m$ is equal to the Langmuir strain constant, S_{max} in this present work. Rewriting this equation results in the following equation for permeability ratio as a function of initial porosity, the Langmuir strain curve constants, and pressure:

$$\frac{k}{k_0} = \left[1 + \left(1 + \frac{2}{\phi_0}\right) S_{max} \left(\frac{p_0}{p_L + p_0} - \frac{p}{p_L + p}\right)\right]^3 . \quad \text{.....(7)}$$

This model neglects the elastic properties of coal and specifies that all permeability changes are caused by sorption-induced strain.

Palmer-Mansoori Model. This is perhaps the most widely discussed permeability model in the literature and other models are based on it. For example, Chikatamarla and Bustin[14] recently published a model that can be shown to reduce to the Palmer-Mansoori model. As with the Seidle-Huitt model, the Palmer-Mansoori model also assumes Reiss's cubic relationship between permeability and porosity for fractured media. The porosity-change equation for this model was given as:

$$\frac{\phi}{\phi_0} = 1 - \frac{1}{M\phi_0}(\sigma - \sigma_0) + \frac{\varepsilon}{\phi_0}\left(\frac{K}{M} - 1\right)\left(\frac{p}{P_L + p} - \frac{p_0}{P_L + p_0}\right). \quad \text{.(8)}$$

where M is the constrained axial modulus, K is the bulk modulus, and ε as the volumetric Langmuir strain constant. Further, the bulk modulus[15] and the constrained axial modulus[6] can be rewritten in terms of Young's modulus and Poisson's ratio; and volumetric Langmuir strain constant is equal to three times the linear Langmuir strain constant:

$$K = \frac{E}{3(1-2\nu)}, \quad M = \frac{E(1-\nu)}{(1+\nu)(1-2\nu)}, \quad \text{and} \quad \varepsilon = 3S_{max},$$

where E is Young's modulus and v is Poisson's ratio. Substituting these values into the porosity equation yields the Palmer-Mansoori permeability equation in terms of Young's modulus, Poisson's ratio, initial porosity, the Langmuir strain curve parameters, and pressure:

$$\frac{k}{k_0} = \left[1 - \frac{(1+\nu)(1-2\nu)}{E(1-\nu)}\frac{(\sigma - \sigma_0)}{\phi_0} + \frac{S_{max}}{\phi_0}\left(\frac{(1+\nu)}{1-\nu} - 3\right)\left(\frac{p}{p_L + p} - \frac{p_0}{p_L + p_0}\right)\right]^3 . \quad \text{.....(9)}$$

All parameters in this equation can be either measured or approximated except the initial porosity, which can have a large effect on the outcome of the model. However, Initial porosity can be obtained by judiciously fitting the above equation to permeability data unaffected by sorption-induced strain and will be discussed later in this paper.

Shi-Durucan Model. This model begins with the derivation for permeability by Seidle et al.[16] as

$$\frac{k}{k_0} = \exp\left[-3C_f(\sigma - \sigma_0)\right], \quad \text{.....(10)}$$

where C_f is the fracture compressibility, and σ is the effective (net) stress. Shi and Durucan then derive an expression for the change in effective stress:

$$\sigma - \sigma_0 = \frac{\nu}{1-\nu}(\sigma - \sigma_0) + \frac{E}{3(1-\nu)}\varepsilon\left(\frac{p}{p_L + p} - \frac{p_0}{p_L + p_0}\right). \quad \text{..(11)}$$

Noting that the volumetric strain, ε, is three times the linear strain and combining the two above equations results in an equation for permeability for the Shi-Durucan model:

$$\frac{k}{k_0} = \exp\left\{-3C_f\left[\frac{\nu}{1-\nu}(\sigma - \sigma_0) + \frac{E}{(1-\nu)}S_{max}\left(\frac{p}{P_L + p} - \frac{p_0}{P_L + p_0}\right)\right]\right\}. \quad \text{.... (12)}$$

The fracture compressibility, C_f, is obtained by judiciously fitting the above equation to permeability data unaffected by sorption-induced strain. However, fracture compressibility is not necessarily constant and we found that a variable compressibility term was better suited to our data. McKee et al.[17] offer the following expression for stress dependent compressibility:

$$C_f = \frac{C_0}{\alpha(\sigma - \sigma_0)}\left\{1 - \exp\left[-\alpha(\sigma - \sigma_0)\right]\right\}. \quad \text{.....(13)}$$

where C_0 is the initial fracture compressibility and α is the fracture compressibility change rate. Substituting this term into the permeability equation yields an an expression for the Shi-Durucan permeability model in terms of fracture compressibility, Young's modulus, Poisson's ratio, the Langmuir strain curve parameters, and pressure:

Experimental Results

Results of the permeability tests are shown as plots of k/k_0 versus pressure. Two cores representing two different coal types were used as well as three different gases (CO_2, CH_4, N_2) with different sorption-induced strain characteristics.

Poisson's ratio and Young's modulus are two of the elastic properties of coal that are needed in order to model the permeability data of coal. Literature values for Poisson's ratio[6,8,16] range from 0.2 to 0.5 for coal. For this work, an average value of 0.35 was assumed. Literature values for Young's modulus[6,8] range from 124,000 psi to 500,000 psi for coal; and for this work, a value of 200,000 psi was assumed.

Varying Overburden Pressure. A series of experiments were conducted where confining (overburden) pressure was varied while holding pore pressure constant with nitrogen as the flowing fluid. These experiments were used to calculate the initial porosity and fracture compressibility constants for each coal core and are reported later in this paper. Because pore pressure was held constant in these experiments, there were no sorption-induced permeability effects, and any gas presumably could have been used with the same results.

To calculate initial porosity and fracture compressibility, the models were fit to the permeability by varying the initial porosity or fracture compressibility constants until a best fit was obtained.

The Seidle-Huitt model is formulated such that if there be no sorption-induced strain (as was the case in this set of experiments), there would be no change in permeability and the permeability ratio would be equal to unity; therefore, this model could not be used to obtain a value for initial porosity. However, the Palmer-Mansoori and Shi-Durucan models can be used to account for changing overburden pressure and were used to obtain initial porosity and fracture compressibility constants. Because the Seidle-Huitt model could not be used to analyze this data set, the Seidle-Huitt initial porosity was set equal to the Palmer-Mansoori initial porosity.

Anderson 01 Core Permeability Data. For the Anderson 01 core, permeability changes resulting from varying the overburden pressure are shown in **Fig. 3**. Along with the actual permeability data, the Palmer-Mansoori and Shi-Durucan models are shown. Because pore pressure was held constant, sorption-induced strain was eliminated, which allowed these data to be used used to calculate the initial porosity and the fracture compressibility constants. These properties of the cores are required by the models in order to be used when pore pressure and sorption-induced strain do affect permeability.

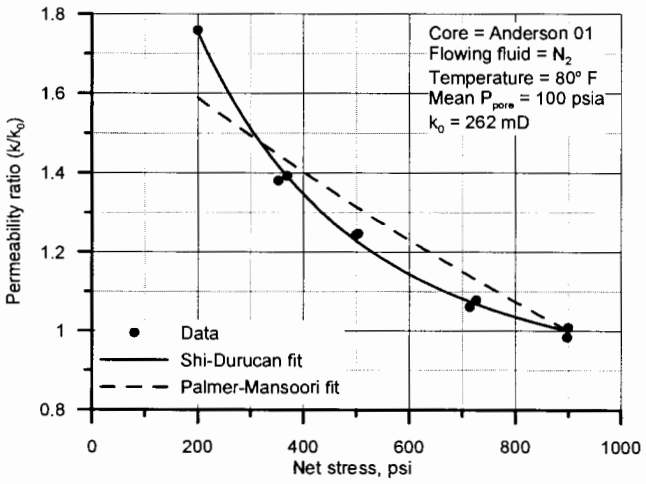

Fig. 3 – Plot showing the permeability changes of the Anderson 01 core as a function on net stress.

Both of these models were forced to a best-fit of the data by varying either the initial core porosity or the core fracture compressibility constants until error was minimized using a least squares process. The calculated initial porosity (using the Palmer-Mansoori model) was 1.31% and the calculated fracture compressibility constants, C_0 and α (using the Shi-Durucan model) were 1.88E-4 psi^{-1} and 24.3E-4 psi^{-1} respectively. If one were to assume fracture compressibility to be constant, a curve similar to the Palmer-Mansoori model would be obtained for the Shi-Durucan model as well.

Gilson 02 Core Permeability Data. For the Gilson 02 core, permeability changes resulting from varying the overburden pressure are shown in **Fig. 4**. Again, two of the models were forced to a best-fit of the data by varying initial porosity and fracture compressibility constants. The calculated initial porosity (using the Palmer-Mansoori model) was 0.804% and the calculated fracture compressibility constants, C_0 and α (using the Shi-Durucan model) were 1.69E-4 psi^{-1} and 37.5E-4 psi^{-1} respectively.

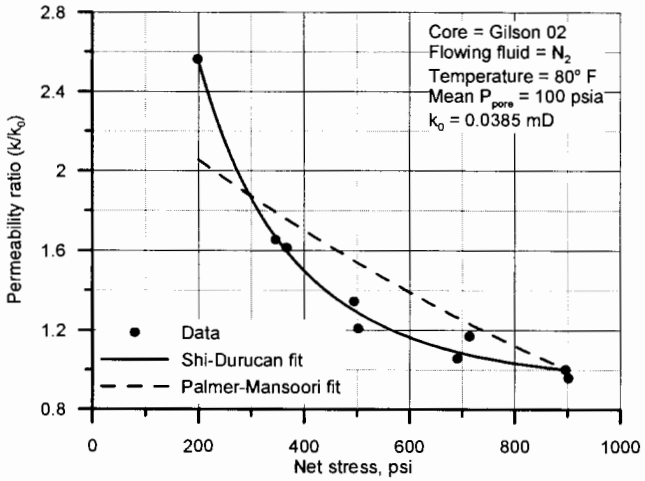

Fig. 4 – Plot showing the permeability changes of the Gilson 02 core as a function on net stress.

Considering the wide difference in permeabilities of these two cores, the calculated fracture compressibilities and porosities were remarkably similar. **Table 3** summarizes the core properties for both the Anderson 01 core and the Gilson 02 core.

Table 3 – Properties of coal cores used in permeability experiments

	Anderson 01	Gilson 02
Rank	Subbituminous	High-volatile bituminous
Vitrinite reflectance, V_r (%)	0.24	0.53
Initial permeability, k_0 (mD)	262	0.0385
Initial porosity, ϕ_0 (%)	1.31	0.804
Average fracture compressibility, C_f, (psi^{-1})	4.17E-4	6.59E-4
Initial fracture compressibility, C_0 (psi^{-1})	1.88E-4	1.69E-4
Fracture compressibility change rate,α (psi^{-1})	24.3E-4	37.5E-4

The values for average fracture compressibility, C_f, obtained in this work (see Table 3) both fall near the lower range of literature values reported for other coals,[16,17] which range from 4.28E-4 psi^{-1} to 18.7E-4 psi^{-1}. The values of compressibility change rate, α, for these two coal cores (see Table 3) compare very closely to a literature value[17] for coal in the Piceance basin equal to 29.5E-4 psi^{-1}.

Varying Pore Pressure. Another series of experiments was conducted where pore pressure was varied while holding constant the confining pressure at 1000 psia. Three different gases (CO_2, CH_4, and N_2) were used as the flowing fluid in these experiments. Because pore pressure was varied, sorption of gases was expected to affect the permeability of the cores to a different degree.

In these experiments, the initial average pore pressure was set to about 100 psia and then increased incrementally until it reached about 800 psia. At each pressure increment, time was given for the gases to adsorb and permeability was monitored until a stable value was achieved.

Anderson 01 Core Permeability Data. Results of varying pore pressure and gas composition for the Anderson 01 coal core are shown in **Fig. 5**. Initial permeabilities, k_0, for all the gases were measured at pore pressures of about 100 psia and are listed in the figure. Even though the same core was used for this set of experiments, the initial permeabilities for each of the gases were different due to the varying amount of sorption-induced strain caused by each of the gases (see Fig. 1). As expected, adsorption of carbon dioxide resulted in the lowest initial permeability (86 mD) for the three gases, followed by methane (147 mD), and nitrogen adsorption resulted in the highest initial permeability (257 mD).

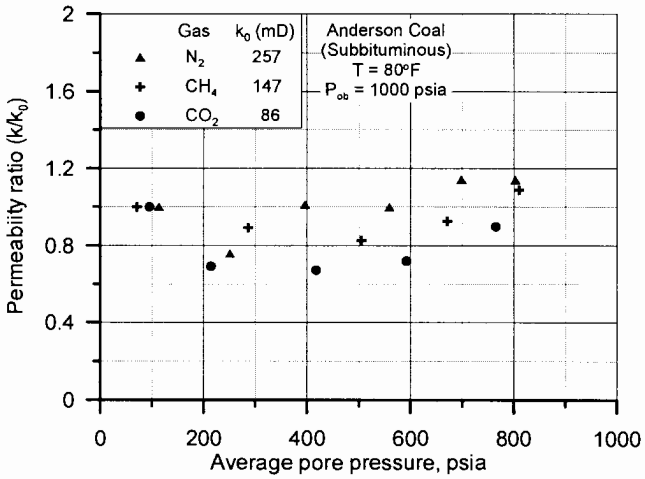

Fig. 5 – Permeability as a function of pore pressure for three gases using the Anderson 01 coal core.

The nitrogen permeability ratio data generally increased as pore pressure increased, signifying very little effect of sorption-induced strain. Increasing the pore pressure (decreasing the net stress) increasingly opened the fractures and increased permeability.

However, the permeability results were different for both methane and carbon dioxide. As pore pressure increased, the permeability initially decreased because of larger sorption-induced strain for these gases compared with nitrogen. Then as pore pressure continued to increase, the permeability also increased because the effect of sorption-induced strain was overcome by the opposite-acting strain caused by the elastic properties of the coal at higher pore pressures.

Gilson 02 Core Permeability Data. Results of varying pore pressure and gas composition for the Gilson 02 coal core are shown in **Fig. 6**. As with the Anderson 01 core, adsorption of carbon dioxide resulted in the lowest initial permeability (0.0226 mD) for the three gases, followed by methane (0.0289 mD), and nitrogen adsorption resulted in the highest initial permeability (0.0372 mD).

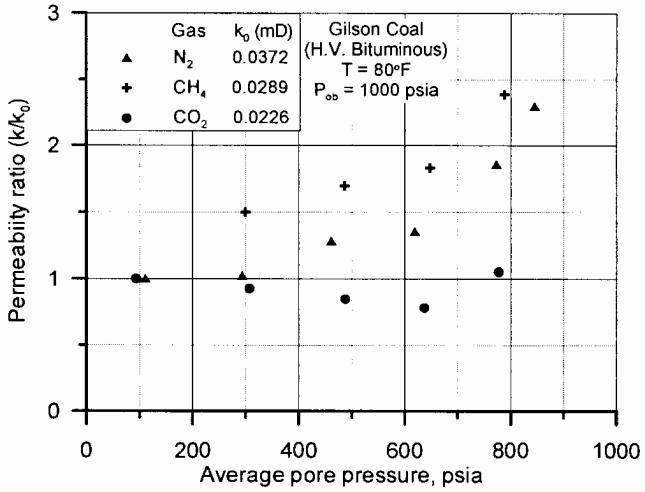

Fig. 6 – Permeability as a function of pore pressure for three gases using the Gilson 02 coal core.

The effect of sorption-induced strain was much less with the Gilson core compared to the Anderson core. This can be attributed to the lower sorption-induced strains associated with the Gilson coal as seen in Fig. 1. The only gas that caused enough sorption-induced strain to decrease the permeability as pore (sorption) pressure increased was carbon dioxide. The sorption of both methane and nitrogen had very little effect on the permeability. The change in permeability with methane and nitrogen for this core can almost entirely be attributed to the cleat compressibility and elastic properties of the coal. For example, the sorption-affected permeability data for nitrogen in Fig. 6 is very similar to the permeability data in Fig. 4, in which there was no gas sorption.

Modeling Sorption-Induced Permeability Changes

The three permeability models discussed earlier were applied to the data shown in Fig. 5 and Fig. 6 to determine how well the models could match permeability data affected by sorption-induced strain. The initial porosity and fracture compressibility constants shown in Table 3 as well as the sorption-induced strain constants were used with the respective models to generate the model output. The plots in **Fig. 7** show the model output along with the original permeability data.

Discussion of Models' Fit of Permeability Data

None of the three coal permeability models did a very good job matching actual permeability data for every case. However, two of the models did relatively well matching the nitrogen permeability data.

Seidle-Huitt Model. This model was designed to predict permeability changes as pore pressure decreased from an initial reservoir pressure towards some lower abandonment pressure as the reservoir was produced. In this paper, we assigned a low initial pore pressure and then increased it. As written, this model specifies that as pore pressure increases, permeability will decrease and sometimes reach negative values. This result is not valid because it does not allow for increasing permeability at higher pore pressure as the data indicate (see

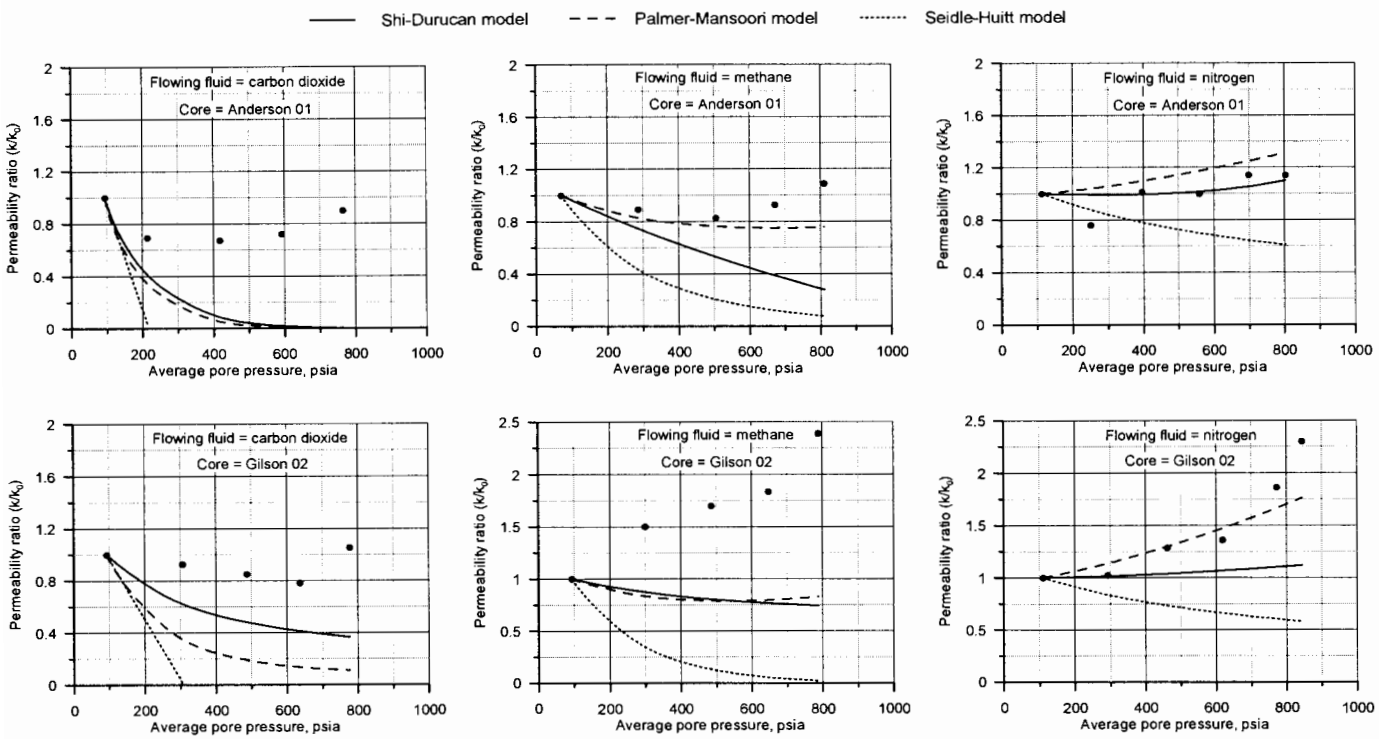

Fig. 7 – Model comparisons for two coal cores and three flowing gases. For all experiments, confining pressure was 1000 psia and temperature was 80° F.

Fig. 7). As a result, this model has a limited range of application.

Because the Seidle-Huitt model neglects the elastic properties of the coal it appears to oversimplify of the mechanics of permeability changes in coal.

Palmer-Mansoori Model. The Palmer-Mansoori model appears to capture many of the trends associated with permeability changes in coal influenced by sorption-induced strain. However, for gases that caused large adsorption strains, this model significantly overestimated the decline in permeability. The Palmer-Mansoori model, as with the Seidle-Huitt model, also has the capability to calculate negative permeability ratios, and interpretive care should be used to not take calculated negative values literally.

Shi-Durucan Model. This model also appears to match some permeability data well, but not all. As with the Palmer-Mansoori model, the Shi-Durucan model tends to overestimate the impact of large sorption-induced strain on permeability. However, with low sorption-induced strain gases, this model is comparable to the Palmer-Mansoori model. In addition, this model is formulated in such a way that the permeability ratio is always greater than zero, which more accurately describes actual permeability data than the other two models.

Application of Correction Factor to Strain Constants. Generally, both the Shi-Durucan model and the Palmer-Mansoori model underestimated the permeability ratio for the six data sets, which begs the question: Is it possible that the unconstrained, sorption-induced strain data we have reported and used are not completely appropriate for the permeability models?

Harpalani and Zhao,[18] Harpalani and Schraufnagel,[19] and Levine[20] all have reported sorption-induced strain data in coal using *unconstrained* coal samples, meaning that the coal samples were allowed to expand in all three directions without applying any external constraining forces. Gray[3] specifically states that unconstrained strain data is appropriate for use in his coal permeability model: "the strain derived from testing samples of coal that are free to move in all directions . . . can be directly used in calculations where strain is related to varying equivalent sorption pressure." Although other modelers[4,6,7,8] do not specifically state that unconstrained strain data is appropriate for use in their models, they do site the unconstrained strain data referenced above, which leads to the conclusion that they, too, believed that the use of unconstrained strain data was appropriate for use in their permeability models.

The data shown in Fig. 7, where measured permeability is compared to model-calculated permeability, indicates that there is less strain occurring during the permeability experiments than that indicated by the measured strain curves. The use of unconstrained sorption-induced strain data in permeability equations designed to model constrained (by overburden pressure) flow tests appears to be somewhat inconsistent. Unconstrained sorption-induced strain data are easily measured and desirable. However, the use of these data in permeability models may need to be modified to account for the constrained nature of the flow tests.

By simply multiplying the strain data by some constant factor, the models can be forced to run through the permeabil-

ity data; however, the shape of the resulting curve does not conform to the data very well, which implies that a variable strain factor that is dependent on pore pressure is needed.

We found that a variable strain factor that is dependent upon the net stress or the pore pressure that has the following form was able to fit the permeability data more closely.

$$S_f = \frac{p_{ob}}{p_p} X, \quad \text{..... (14)}$$

where p_{ob} is the overburden pressure (psi), p_p is the pore pressure (psi) and X represents a factor that is different for each permeability data set and was determined by fitting the model output to the permeability data using a least squares analysis.

We next found that for both the Palmer-Mansoori and the Shi-Durucan models, a grouping of pertinent strain, coal, and gas parameters had a very good linear relationship with the calculated values for X. The resulting linear relationship was determined to be:

$$X = a + b\left(\frac{p_L}{S_{max} V_r^{\,2} \sqrt{\gamma}}\right), \quad \text{..... (15)}$$

where P_L and S_{max} are the Langmuir strain parameters, V_r is the vitrinite reflectance for the coal, and γ is the specific gravity of the gas. The constants 'a' and 'b' in Eq (15) are unique for each of the two models. For the Shi-Durucan model the values for 'a' and 'b' are 8.6846E-2 and 8.4787E-8 psi^{-1} respectively. For the Palmer-Mansoori model the values for 'a' and 'b' are 12.609E-2 and 15.346E-8 psi^{-1} respectively. By combining Eq (14) and Eq (15), we obtained an expression for a variable strain factor (S_f) that when multiplied to the Langmuir strain constant, S_{max}, improves both models' ability to match the actual permeability data:

$$S_f = \frac{p_{ob}}{p_p}\left[a + b\left(\frac{p_L}{S_{max} V_r^{\,2} \sqrt{\gamma}}\right)\right]. \quad \text{..... (16)}$$

Fig. 8 shows the output of the Palmer-Mansoori model and the Shi-Durucan model when the variable strain factor is applied to the original unconstrained strain data and the permeability data for the two coal cores and three gases. Compared to the models' results shown in Fig. 7, the results when the variable strain factor is applied (Fig. 8) are much better for all coals and gases.

Testing the Strain Modification. To test the modification to the strain data, two new data sets were collected using a gas mixture for both coal cores. The gas mixture, as confirmed by GC analysis, was 51% nitrogen and 49% carbon dioxide. Sorption-induced strain measurements were taken and used to calculate the Langmuir strain constants shown in **Table 4**.

Table 4 – Langmuir constants for sorption-induced strain curves for a gas mixture at 80° F.

Gas	Coal	Constants for Strain Curves		R^2 value for curve fit
		Normalized S_{max}	Average p_L, psia	
51% N_2 – 49% CO_2	Anderson	0.01766	306.27	0.9952
	Gilson	0.00844		0.9985

The permeability data for each core was collected in the same manner as the previous permeability experiments with

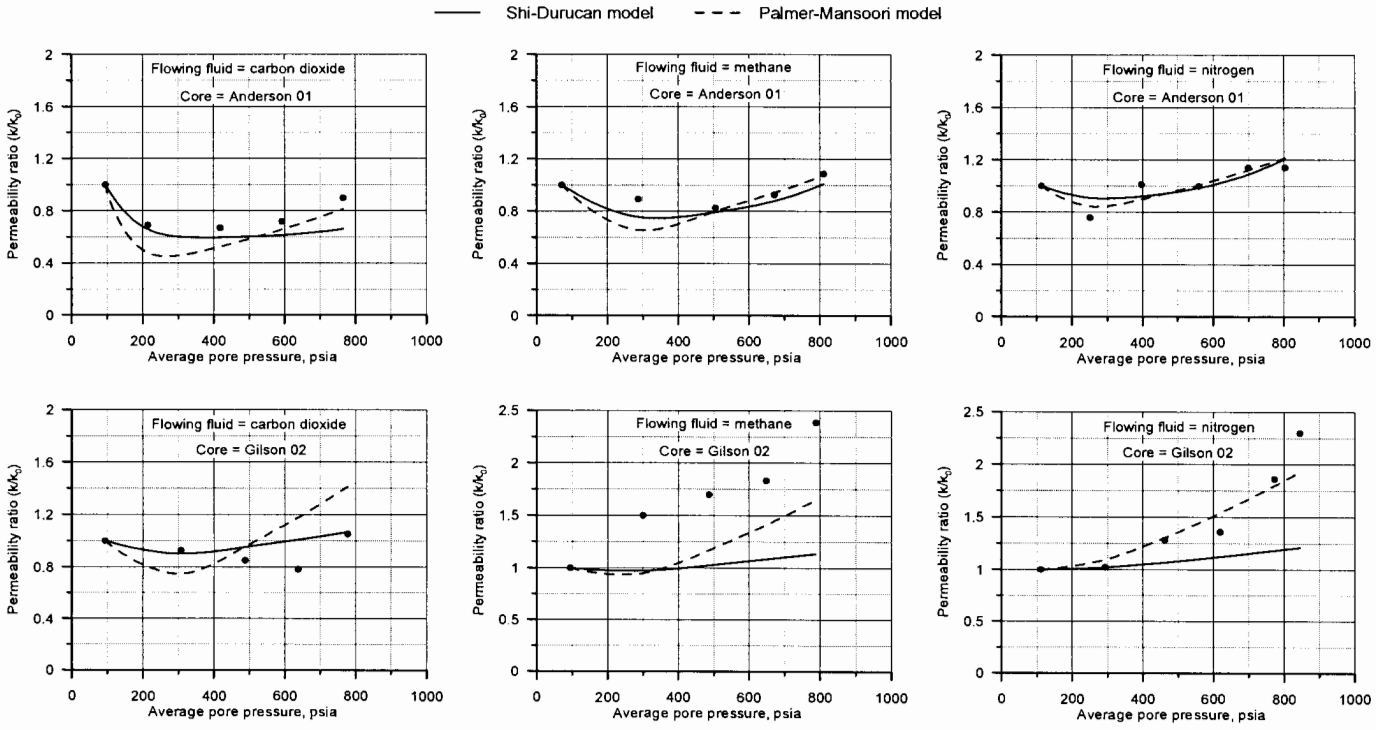

Fig. 8 – Plots showing refined model comparisons for two coal cores and three flowing gases. For all experiments, confining pressure was 1000 psia and temperature was 80° F.

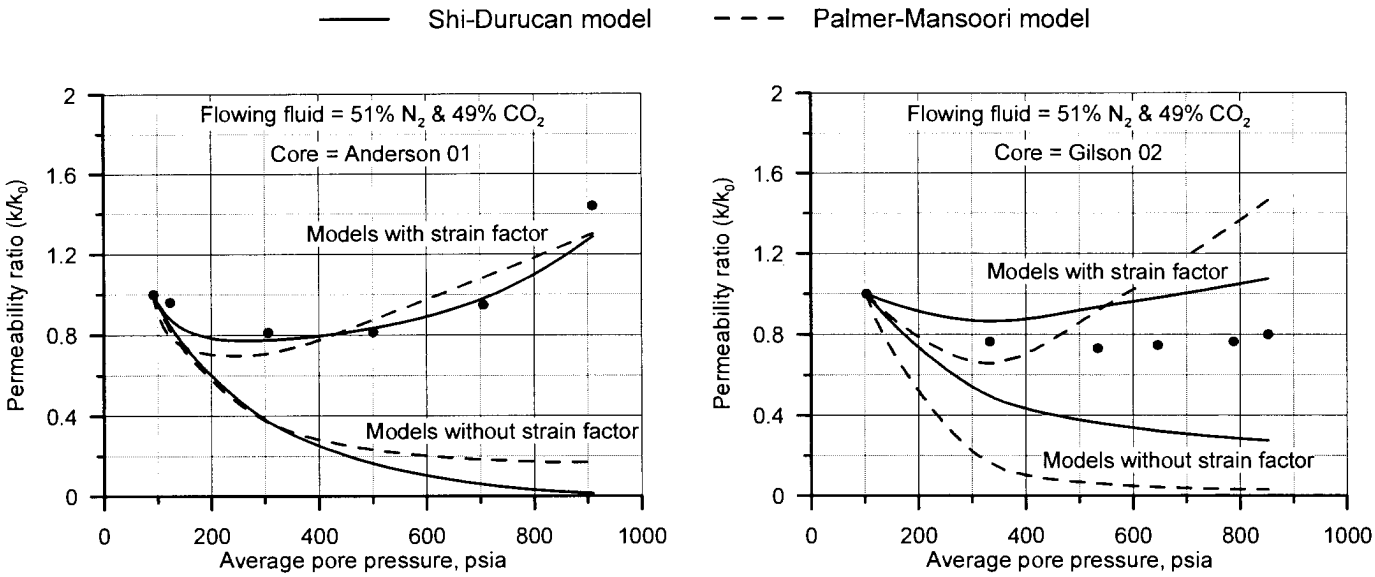

Fig. 9 – Plots showing permeability model comparisons for a gas mixture flowing through two coal cores. Confining pressure was 1000 psia and temperature was 80° F.

the exception of the composition of the gas flowing through the cores. The same gas mixture that was used in the strain experiments was employed for the permeability tests. **Fig. 9** shows the generated permeability data along with the original models and the models using the variable strain factor for these two cores.

Incorporating the variable strain factor to both of the models greatly improved the capability to fit the permeability data for the Anderson 01 core. For the Gilson 02 core, the results were not as striking, but still did improve the fit of the data, especially for the Palmer-Mansoori model. These results tend to validate the assumption that unconstrained strain data need to be adjusted in order to be used to fit actual permeability data.

Conclusions

Some important conclusions can be drawn from the work presented in this paper.

Although there are many models available for use in predicting coal permeability changes as a function of pore pressure, some are too simplistic to be of real value in reservoir simulation

The models considered here significantly overestimated the decrease in permeability as pore pressure was increased.

Because strain measurements were taken on unconstrained coal samples, there may be a need to apply a correction factor to the strain data in order to apply the data to constrained laboratory cores or to field permeability measurements.

A correction factor has been developed that is a function of pore pressure, overburden pressure, gas type, and coal rank that when multiplied to the original strain data, improves both the Palmer-Mansoori model and the Shi-Durucan model.

A test of the correction factor using a gas mixture appears to validate the application of the correction factor to the strain data.

Nomenclature

- a = constant used in variable strain factor equation, dimensionless
- b = constant used in variable strain factor equation, psi^{-1}
- C_f = fracture compressibility, psi^{-1}
- C_0 = initial fracture compressibility, psi^{-1}
- E = Young's modulus, psi
- k = permeability, mD
- k_0 = initial permeability, mD
- L = length, cm
- ΔL = change in length, cm
- M = constrained axial modulus, psi
- p = pressure, psia
- p_L = Langmuir pressure constant, psia
- p_0 = initial pressure, psia
- p_{ob} = overburden pressure, psia
- p_p = pore pressure, psia
- R^2 = coefficient of determination, dimensionless
- S = strain, dimensionless
- S_f = variable strain factor, dimensionless
- S_L = linear strain, dimensionless
- S_{max} = Langmuir linear strain constant; strain at infinite pressure, dimensionless
- S_V = volumetric strain, dimensionless
- V = volume, cm^3
- ΔV = change in volume, cm^3
- V_r = vitrinite reflectance, %
- X = interim strain factor, dimensionless
- α = fracture compressibility change rate, psi^{-1}
- γ = gas gravity, dimensionless
- ε = volumetric strain, dimensionless
- ν = Poisson's ratio, dimensionless
- σ = net stress, psi
- σ_0 = initial net stress, psi
- ϕ = porosity, dimensionless
- ϕ_0 = initial porosity, dimensionless

SI Metric Converstion Factors

psi	× 6.894 757	E + 00	= kPa
in.	× 2.54*	E + 00	= cm
Btu	× 1.055 056	E + 00	= kJ
ft	× 3.048*	E – 01	= m
lbm	× 4.535 924	E – 01	= kg
°F	(°F – 32)/1.8		= °C

* Conversion factor is exact.

Acknowledgments

This work has been funded by Battelle Energy Alliance, the prime contractor at Idaho National Laboratory. The authors wish to express their thanks to the management of Idaho National Laboratory for funding this work and allowing its publication. We also express our gratitude to Mike Glasson of Andalex Resources and Greg Gannon of Kennecott for help in the collection of the coal samples.

References

1. Berkowitz, N.: *Coal Science and Technology 7 – The Chemistry of Coal*, Elsevier Science (1985) 86.
2. "RECOPOL Workshop," *Greenhouse Issues*, Number 78 (June 2005) 5-7, www.ieagreen.org.uk.
3. Gray, I.: "Reservoir Engineering in Coal Seams: Part 1 – The Physical Process of Gas Storage and Movement in Coal Seams," paper SPE 12514, *SPE Reservoir Engineering* (February 1987) 28-34.
4. Sawyer, W.K., G.W. Paul, and R.A. Schraufnagel: "Development and Application of a 3D Coalbed Simulator," paper CIM/SPE 90-119, presented at the 1990 International Technical Meeting hosted jointly by the Petroleum Society of CIM and the Society of Petroleum Engineers, Calgary, Alberta, Canada (10-13 June 1990).
5. Seidle, J.P. and L.G. Huitt: "Experimental Measurement of Coal Matrix Shrinkage Due to Gas Desorption and Implications for Cleat Permeability Increases," paper SPE 30010, presented at the 1995 International Meeting on Petroleum Engineering, Beijing, China (14-17 November 1995).
6. Palmer, I. and J. Mansoori: "How Permeability Depends on Stress and Pore Pressure in Coalbeds: A New Model," paper SPE 52607, *SPE Reservoir Evaluation & Engineering* (December 1998) 539-544.
7. Pekot, L.J. and S.R. Reeves: "Modeling the Effects of Matrix Shrinkage and Differential Swelling on Coalbed Methane Recovery and Carbon Sequestration, paper 0328 *proc.* 2003 International Coalbed Methane Symposium, University of Alabama, Tuscaloosa, Alabama (May 2003).
8. Shi, J.Q. and S. Durucan: "Changes in Permeability of Coalbeds During Primary Recovery – Part 1: Model Formulation and Analysis," paper 0341 *proc.* at the 2003 International Coalbed Methane Symposium, University of Alabama, Tuscaloosa, Alabama (May 2003).
9. Stricker, G.D. and M.S. Ellis: "Coal Quality and Geochemistry, Powder River Basin, Wyoming and Montana," 1999 Resource Assessment of Selected Tertiary Coal Beds and Zones in the Northern Rocky Mountains and Great Plains Region, Part I: Powder River Basin, *in* U.S. Geological Survey Professional Paper 1625-A (1999).
10. *Annual Review and Forecast of Utah Coal, Production and Distribution – 2003*, prepared by the Utah Energy Office, Department of Natural Resources (October 2004).
11. Robertson, E.P. and R.L. Christiansen: "Optically-based Strain Measurement of Coal Swelling and Shrinkage," paper 0417 *proc.* 2004 International Coalbed Methane Symposium, University of Alabama, Tuscaloosa, Alabama (May 2004).
12. Robertson, E.P. and R.L. Christiansen: "Measurement of Sorption-Induced Strain," paper 0532, *proc.* 2005 International Coalbed Methane Symposium, University of Alabama, Tuscaloosa, Alabama (May 2005).
13. Reiss, L.H., *The Reservoir Engineering Aspects of Fractured Formations*, Gulf Publishing Company, 1980.
14. Chikatamarla, L. and M.R. Bustin: "Implications of Volumetric Swelling/Shrinkage of Coal in Sequestration of Acid Gases," paper 0435, *proc.* 2004 International Coalbed Methane Symposium, University of Alabama, Tuscaloosa, Alabama (May 2004).
15. *Petroleum Engineering Handbook*, H.B. Bradley (ed.), third printing, Society of Petroleum Engineers, Richardson, Texas (1992) 51-2.
16. Seidle, J.P., M.W. Jeansonne, and D.J. Erickson: "Application of Matchstick Geometry to Stress Dependent Permeability in Coals," paper SPE 24361 presented at the SPE Rocky Mountain Regional Meeting, Casper, Wyoming (18-21 May 1992).
17. McKee, C.R. A.C. Bumb, and R.A. Koenig: "Stress-Dependent Permeability and Porosity of Coal and Other Geologic Formations," paper SPE 12858, *SPE Formation Evaluation* (March 1988) 81-91.
18. Harpalani, S. and X. Zhao: "Changes in Flow Behavior of Coal with Gas Desorption," paper SPE 19450, unsolicited manuscript (1989).
19. Harpalani, S. and R.A. Schraufnagel: "Influence of Matrix Shrinkage and Compressibility on Gas Production From Coalbed Methane Reservoirs," paper SPE 20729, *proc.* 1990 SPE Annual Technical Conference and Exhibition, New Orleans, Louisiana (23-26 September 1990).
20. Levine, J.R.: "Model study of the influence of matrix shrinkage on absolute permeability of coal bed reservoirs," *Coalbed Methane and Coal Geology*, R. Gayer and I. Harris (eds), Geological Society Special Publication No. 109 (1996) 197-212.